Materials Chemistry and Physics 122 (2010) 537–543

Contents lists available at ScienceDirect

Materials Chemistry and Physics

journal homepage: www.elsevier.com/locate/matchemphys

High temperature chemical and physical changes of the HVPE-prepared GaN semiconductor

Mariusz Drygas[a], Miroslaw M. Bucko[b], Zbigniew Olejniczak[c], Izabella Grzegory[d], Jerzy F. Janik[a,*]

[a] AGH University of Science and Technology, Faculty of Energy and Fuels, al. Mickiewicza 30, 30-059 Krakow, Poland
[b] AGH University of Science and Technology, Faculty of Materials Science and Ceramics, al. Mickiewicza 30, 30-059 Krakow, Poland
[c] Institute of Nuclear Physics, Polish Academy of Sciences, ul. Radzikowskiego 152, 31-342 Krakow, Poland
[d] Institute of High Pressure Physics - Unipress, Polish Academy of Sciences, ul. Sokolowska 29/37, 01-142 Warszawa, Poland

ARTICLE INFO

Article history:
Received 30 September 2009
Received in revised form 10 March 2010
Accepted 16 March 2010

Keywords:
Gallium nitride
GaN
HVPE
Stability
XRD
NMR
TGA

ABSTRACT

Samples of HVPE-prepared hexagonal gallium nitride GaN were subjected to high temperatures under ammonia in order to induce decomposition. Powder XRD, SEM, and solid-state ^{69}Ga and ^{71}Ga MAS NMR spectroscopy were used to characterize changes in structure and morphology. The major changes were found to include GaN sublimation and decomposition to the elements in the gas phase. No significant Knight shift effect was detected by gallium NMR in striking contrast to the behavior observed earlier in a similar study of GaN nanopowders. The latter could now be linked to crystal growth and recrystallization phenomena that operate efficiently in pyrolyzed nanopowders while being absent or negligible in heated polycrystalline HVPE materials.

1. Introduction

The impacts of gas atmosphere, temperature, and pressure conditions on the powder processing and ultimate performance characteristics of the modern semiconductor gallium nitride, GaN [1] are poorly defined. In fact, prior work from our laboratory [2] indicates that there are important unanswered questions surrounding the thermal stability range under various gas atmospheres, the structural basis for thermally induced nitrogen deficiency/vacancies and resulting electronic phases, and the interrelationship of decomposition and sublimation for different morphologies.

In this regard, both we and others have reported studies of intriguing structural and electronic changes in a variety of hexagonal [3–5] and cubic (zinc blende) [5] GaN nanopowders stressing the often equivocal information derived from investigations by using powder XRD and solid-state NMR techniques. Specifically [3], the ^{69}Ga MAS NMR spectroscopy for the nanopowders prepared and pyrolyzed under various temperature/time conditions exhibited two types of responses. A high-frequency Knight-shifted resonance, that appeared with higher pyrolysis temperatures and/or extended pyrolysis times, was assigned to decomposition-induced N-deficient domains, and it was often dominate or exclusive compared to a low-frequency resonance for stoichiometric GaN (Ga(4N) chemical environments). At the same time, the materials showed by powder XRD the crystalline GaN polytypes encompassing mostly single ordered/disordered hexagonal GaN and after higher pyrolysis temperatures yielded products of better and better crystallinity. This trend could be tentatively explained by assuming that the scarce N-deficient sites (*e.g.*, oxygen dopant stabilized defects or other native N-defects) resulting from partial decomposition or dopant incorporation reactions of GaN form a structural basis for the electronic phase with conduction electrons. The latter are responsible for the observed Knight shift effect and the altered materials properties. Herein, we report parallel studies of polycrystalline GaN powders obtained by grinding monocrystalline epitaxial GaN prepared by Hydrogen Vapor Phase Epitaxy (HVPE). Such materials show a significantly different behavior at high temperatures compared with the nanopowders.

2. Experimental

2.1. Materials

Translucent platelets of epitaxial GaN (thickness 0.5–0.7 mm) were prepared by hydride/halide vapor phase epitaxy (HVPE) at 1100 °C on native GaN substrates in two different runs providing materials for Sample 1 and Sample 2 (Unipress, Warsaw, Poland). One run produced an intentionally Si-doped GaN sample at the

* Corresponding author. Tel.: +48 126172577.
E-mail address: janikj@agh.edu.pl (J.F. Janik).

0254-0584/$ – see front matter © 2010 Elsevier B.V. All rights reserved.
doi:10.1016/j.matchemphys.2010.03.043

level of 10^{18} cm^{-3} (Sample 2). All samples were unintentionally doped with oxygen and iron at much lower levels. The doping aspect was considered not essential for the scope of this study. The powder samples were obtained by grinding bulk platelets by hand in an agate mortar. The resulting rather coarse powders had particles sizes spanning from a few to a few hundred microns (SEM observations) and, therefore, were in the microcrystalline size range. An eye-ball estimation of the SEM pictures indicated a higher ratio of the finest grain fraction in ground Sample 1 compared with ground Sample 2 (*vide infra*).

2.2. Heating treatment and products

The samples contained in an alumina crucible were heated in a tube furnace at 10 °C min^{-1} under an ammonia flow to reach a final pyrolysis temperature, first 1250 °C and then 1300 °C, and maintained at each level for several hours. Upon cooling to room temperature, the samples were checked for changes by powder XRD and ^{69}Ga and ^{71}Ga MAS NMR. The heating was subsequently continued at 1300 °C until the diminishing mass of remaining material enabled its spectroscopic characterization. The heating scheme is summarized in Table 1. After completing the project, coarse deposits were observed in the vicinity of the crucible zone inside the furnace tube. This material (~0.2 g) was recovered as shiny dark platelets and elongated crystallites. Traces of powdery black films were also observed at the tube exit.

2.3. Characterization

All products were characterized by standard powder XRD analysis (X'Pert Pro Panalytical, Cu K_α source; 2θ = 20–80°). Each powder sample was placed in a metal support and pressed by applying a normal force and shear motion to make the surface of the powder mount smooth and flat. Solid-state ^{69}Ga and ^{71}Ga MAS NMR spectra were measured on an APOLLO console (Tecmag) at the magnetic field of 7.05 T produced by a 89 mm bore superconducting magnet (Magnex). A Bruker HP-WB high-speed MAS probe equipped with a 4 mm zirconia rotor and KEL-F cap was used to record the MAS spectra at the spinning rates of 8.5 or 13 kHz. The ^{69}Ga and ^{71}Ga spectra were measured at 71.925 and 91.385 MHz, respectively, using a single 2 μs rf pulse, which corresponded to $\pi/4$ flip angle in the liquid. The acquisition delay used in accumulation was 5 s and the typical number of acquisitions was 400. The frequency scale in ppm was referenced to the resonances of $Ga(NO_3)_3$ (1 M in D_2O). All resonance positions were uncorrected for the second order quadrupolar shift. To identify the spinning sidebands, data were recorded at two spinning rates, *i.e.*, 8.5 and 13 kHz. Because of limited bandwidths of the MAS probe and the NMR receiver, the signal from metallic Ga was searched by a systematic change of the resonance offset in the NMR console, paralleled by the corresponding retuning of the probe. Once the NMR signal from metallic β-Ga was detected at the 0.45% Knight shift (no signal was detected in the Knight shift range expected for α-Ga) [6], the NMR spectrum was measured using the same acquisition parameters as in the normal frequency range. SEM micrographs were acquired with a Hitachi Model S-4700 scanning electron microscope. FT-IR spectra for KBr pellets were recorded with a Nicolet 380 (Thermo Electron Corp.). TGA/DTA scans were measured on a TA Instruments STA-SDT 2960 apparatus (disposable Al_2O_3 crucibles, helium UHP 5N, sample mass 20–40 mg, helium purge before determinations at 30 °C for 1 h, heating rate 10 °C min^{-1}).

3. Results and discussion

Ground samples of HVPE GaN were heated under NH_3 at 1250 °C for 4 h followed by consecutive stages at 1300 °C (Table 1). The bulk platelet of Sample 1 was heated under less demanding conditions, *i.e.*, 1 h at 1250 °C and 1 h at 1300 °C in order to examine the early stages of mass losses. In this regard, a 3-h heating at 1300 °C of a single small-sized platelet (few mm^2) resulted in its complete disappearance from the crucible. The total length of heating at 1300 °C was guided at first by visual changes of sample appearance (darkening) after a given stage followed by XRD and NMR investigations to detect potential long and/or short range structural changes. When no essential changes in NMR were seen, the heating was continued.

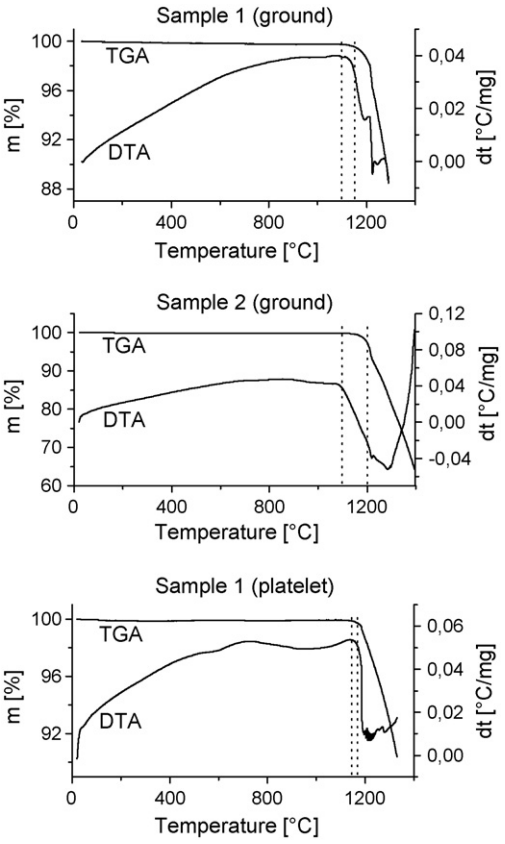

Fig. 1. TGA/DTA determinations for HVPE GaN under helium.

Eventually, after reaching a certain stage, a drastic mass loss was observed for each sample and the experiment was terminated. No metallic gallium was found in the crucibles containing the heated products. In this regard, Sample 1 appeared to be much more prone to changes already after 6 h at 1300 °C to be compared with more than double this time for Sample 2 that yielded similar mass losses. Somewhat different local diffusion/mass transfer conditions in the former case, associated with a smaller mass of Sample 1 and its specific grain sizes after an apparent deeper grounding, could at least partially be responsible for the effect.

3.1. TGA/DTA under helium

The TGA/DTA traces under UHP helium for all samples are shown in Fig. 1. For each sample, one can assign the on-set temperature for an endothermic event from the respective DTA curve and an approximate decomposition temperature from the TGA curve, *i.e.*, Sample 1 (ground), 1100 and 1150 °C, Sample 1 (platelet), 1140 and 1170 °C, and Sample 2 (ground), 1100 and 1200 °C, respectively. It is apparent that the decomposition behaviors under helium vary somewhat among the samples. For instance, the bulk platelet of Sample 1 is a bit more resistant than its ground powder. For all

Table 1
Scheme for heating under ammonia of HVPE GaN.

	Sample 1 (ground)	Sample 1 (platelet)	Sample 2 (ground)
Initial mass [g]	0.3203	0.0092	0.5723
Heating stages: temperature, time (stage mass loss)			
Stage 1	1250 °C, 4 h followed by 1300 °C, 4 h (54.0 wt%)	1250 °C, 1 h followed by 1300 °C, 1 h (6.5 wt%)	1250 °C, 4 h followed by 1300 °C, 6 h (5.6 wt%)
Stage 2	1300 °C, 2 h (71.2 wt%)		1300 °C, 6 h (37.6 wt%)
Stage 3			1300 °C, 3 h (89.8 wt%)

the materials, the on-set of the endothermic effect is found consistently around 1100 °C with decomposition evident near 1200 °C. The latter values are significantly higher by 100–200 °C compared with the decomposition temperatures of 930–1050 °C observed for a large number of GaN nanopowders in our previous study [3] and in other related thermogravimetric studies of GaN [7]. The initial low temperature weight losses for the HVPE samples before decomposition (*ca.* 0.2 wt%) are much lower than those observed for the nanopowders (even up to 3 wt%). It is worth pointing out that metallic gallium was recovered in the crucibles after the measurements supporting a rather fast endothermic decomposition in bulk as the major phenomenon responsible for the mass loss under applied conditions.

3.2. XRD study

The XRD patterns for ground Sample 1 and ground Sample 2 (Table 1) are shown in Fig. 2. All materials are phase pure hexagonal GaN with cell parameters close to the reference values indicating that good crystallinity persists through the heating stages [8]. Diffraction peak intensities support a highly textured nature of crystallites; however, due to incidental grain size and shape specifics after grinding and, additionally, rather uncontrolled grain alignment during XRD sample preparation, it is hard to draw any clear-cut conclusions regarding specific/preferred crystallite decomposition directions. In this regard, it is worth mentioning that in all the patterns, and independently on other diffraction intensities, a significant reduction in the relative (0 0 2) diffraction intensity is usually observed. This could indicate that, other things being equal, preferential initial grain orientation perpendicular to the *z*-axis eventually diminishes with heating. The SEM and NMR examinations of the heated products provide additional confirmation of such grain morphology evolution shedding some more light into this question (*vide infra*).

Fig. 3 includes the XRD patterns for the deposit from the furnace heating tube. The pattern for the as-recovered material (platelets, long whiskers) confirms it as the highly textured microcrystalline GaN, this time with a visibly enhanced (0 0 2) diffraction intensity. The textured morphology apparently results from the perpendicular to the *z*-axis preferential/aligned grain growth on the tube's surface since the pattern for the sample that was later ground indicates a much better homogenous/random crystallite distribution. The FT-IR spectrum for the material (not shown) also confirms it as gallium nitride; in addition, no Ga–O stretches were detected.

3.3. Solid-state ^{69}Ga and ^{71}Ga MAS NMR determinations

There are two stable isotopes of gallium occurring in nature, *i.e.*, ^{69}Ga and ^{71}Ga with natural abundances *ca.* 60% and 40%, respectively, both possessing nuclear spin 3/2. Therefore, the MAS NMR spectra of both isotopes are broadened by the second order quadrupolar interaction. Despite its lower natural abundance, the ^{71}Ga MAS NMR is more sensitive due to higher resonance frequency and usually yields narrower spectra because it has a smaller quadrupolar moment. For both isotopes, the resonance positions in various GaN materials practically differ only by several ppm in a range 300–500 ppm measured relative to 1 M $Ga(NO_3)_3$ /D_2O solution. Shifts are usually quoted uncorrected for the second order quadrupolar shifts [3–5]. The Knight-shift effect linked to the presence of conduction electrons appears to be responsible for the sometime observed resonance evolution and shifting to higher frequencies in some GaN materials [3,4f, 4g, 5a]. Although the exact structural/compositional origin of the conduction electrons is still a subject of debate, the appearance and increased intensity of the Knight-shifted resonance after high temperature and long time treatments of pure (not intentionally doped) GaN nanopowders

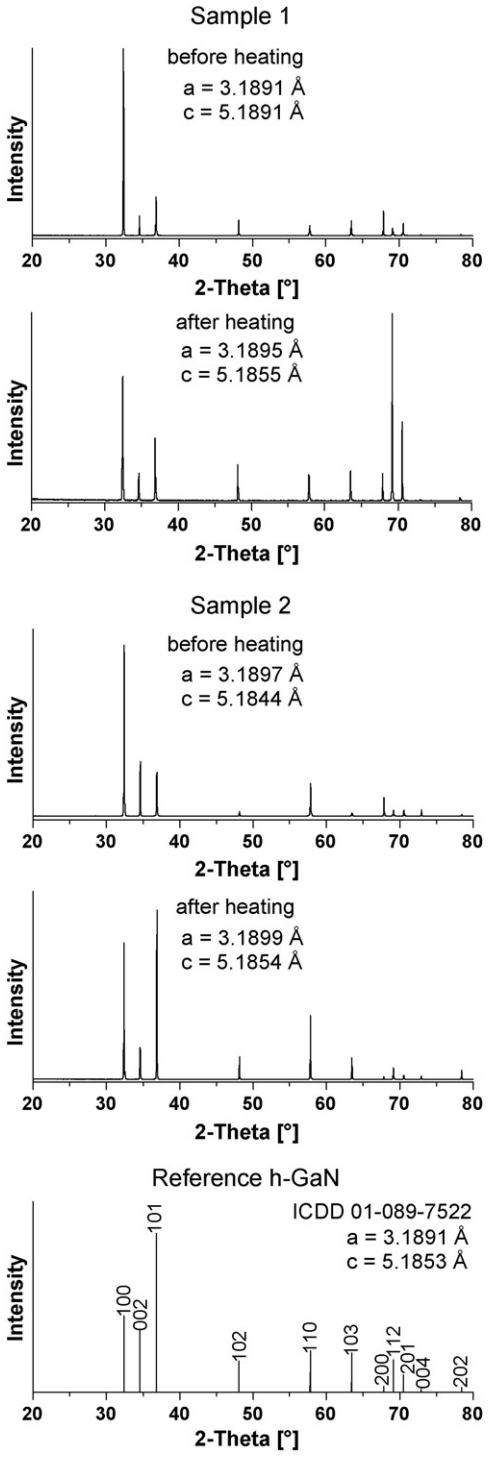

Fig. 2. XRD patterns of the ground HVPE GaN materials.

seem to provide useful guidelines as to approaching the limits of the materials temperature *vs.* time structural integrity.

Fig. 4 shows the ^{69}Ga and ^{71}Ga MAS NMR spectra for ground Sample1 and Sample 2.

It is clear that after the 4-h treatment at 1300 °C of Sample 1 (Fig. 4A), a weak and very broad resonance at *ca.* 410–420 ppm in the ^{69}Ga NMR spectrum and at *ca.* 430–440 ppm in the ^{71}Ga NMR spectrum appears to accompany the major peak for stoichiometric GaN which is located in the 300 ppm range. Additionally, small quantities of metallic gallium are responsible for a weak res-

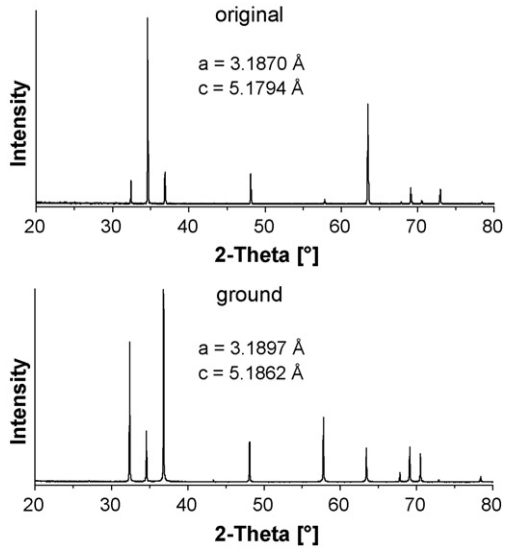

Fig. 3. XRD patterns of the crystalline deposit recovered from the heating tube.

onance observed at *ca.* 0.45% in this material. On the other hand, no such additional resonances are evident in the spectra for Sample 2 heated under similar conditions for a much longer period of time (15 h) (Fig. 4B). Recall that the higher-frequency resonance was convincingly proposed to result from the Knight shift effect in the semiconductor (*vide infra*). It seems, therefore, that Sample 1 decomposes faster and slightly differently than Sample 2. It is suggested that there is transient formation of an electronic N-deficient phase responsible for conduction electrons as well as some small quantities of retained metallic Ga. Regarding this, no bulk metallic gallium was seen by eye in the crucible after the completion of any of the heating stages.

A detailed comparison of the central transition line shape in the ^{71}Ga NMR spectra for the two materials is presented in Fig. 4C. This includes, for clarity, only the limiting spectra acquired for the materials before and after the final heating. It is found that the width and position of the resonance peak after each of the consecutive heating stages remain practically unchanged indicating a high stability of the electric field gradient tensor parameters in the Ga(4N) environment of the stoichiometric GaN lattice. Such behavior supports a highly stable nature of the crystal field and corresponds with good crystal quality of GaN contained in the heated products. Further, the high-frequency shoulder increases so that the shape of the spectrum approaches the theoretical asymmetric doublet [9]. Parallel changes are observed in an identical manner in the respective ^{69}Ga MAS NMR spectra shown in Fig. 4D. A detailed analysis of the spectra confirms that changes of the spin-lattice relaxation time T_1 are responsible for this effect, *i.e.*, T_1 becomes shorter and shorter upon heating. These observations can be reasonably explained by assuming that each subsequent heating stage yields more and more textured crystallites surviving the treatment. In this regard, those crystallites that are smaller and with multiple surfaces should decompose and/or sublime in the first place leaving behind the larger grains with a more pronounced textured morphology (*vide infra*, SEM examination). This increases the overall surface area of the material and contributes to enhanced T_1 relaxation.

3.4. SEM examination

The SEM micrographs for ground Sample 1 after heating (Fig. 5B–D) typically show a textured and quite aligned fibrous morphology of many grains. This is consistent with mass transfer phenomena (decomposition and/or sublimation) along certain preferred directions, *i.e.*, perpendicular to the fibers length. There are also grains with pit-like features on some grain surfaces commonly observed by us for gas-etched GaN crystallites (Fig. 5D). Very much the same morphology emerges from the SEM examination of Sample 2 (not shown) although it seemed to consist of coarser grains than Sample 1.

The SEM pictures for the heated bulk platelet of Sample 1 (Fig. 6B–D) show the quite deep pits (Fig. 6B) accompanied by developing and somewhat aligned shallow rifts on the otherwise smooth surface (Fig. 6C). Since the surface of the platelet corresponds to a plane perpendicular to the *z*-axis of the epitaxial GaN crystal, the progressing evolution of the rifts could lead, eventually, to the fibrous appearance seen in the more heated grains. There are also small regions with spheroidally shaped features suggesting partial melting (Fig. 6D). Interestingly, EDX analyses of such features show a significant relative enrichment in oxygen and gallium *vs.* nitrogen.

The shiny deposits recovered from the reaction tube were found by XRD and FT-IR (*vide intra*) to consist mostly of microcrystalline hexagonal GaN. Fig. 7 presents the SEM pictures of typical morphologies in this material. In addition to several well-faceted single crystals of GaN (*e.g.*, Fig. 7A, upper right-hand corner), there are lumps of polycrystalline materials of homogeneous morphology containing much smaller aligned crystallites (Fig. 7B, magnification of the lowest positioned agglomerate in Fig. 7A). Few other agglomerates consist of an apparent shapeless bulk support with quite numerous spheroidal features embedded in it (Fig. 7C); these agglomerates are found by EDX to be gallium enriched consistent with them containing some metallic Ga. Some of these gallium-rich regions show numerous several micrometer long and regularly faceted GaN whiskers grown on them as seen in Fig. 7D (magnification of the agglomerate furthest to the right in Fig. 7A).

3.5. Thermal stability of HVPE GaN

Perhaps the most obvious observation of this study is, in general terms, a much better resistance to high temperatures under different gas atmospheres of the epitaxial HVPE GaN, both ground (polycrystalline in the microcrystallinity range) and in bulk platelets (monocrystalline), compared to a wide range of the previously investigated nanocrystalline powders of GaN. First, under the conditions of the TGA/DTA experiment (helium flow, relatively very small samples, continuous heating rate of 10 °C min^{-1}) the observed rather abrupt mass losses are mostly due to decomposition of GaN to the elements and take place for the HVPE materials in the 1100–1200 °C range, *i.e.*, at higher temperatures of up to 200 °C than for the nanopowders [3]. In our opinion, the better crystallinity and much lower surface areas of the ground HVPE GaN samples compared with the as-synthesized nanopowders are, likely, the major factors behind such a behavior. Second, various raw GaN nanopowders in our hands, after heating under an ammonia flow already at 975–1000 °C for several hours, showed mass losses of the order of 20–40 wt% that were accompanied by significant crystal growth/recrystallization, resublimation with long GaN whisker formation on crucible edges, and decomposition to the elements including Ga metal formation within the powder bulk and in the crucible's bottom as well as fine metal deposits on the surface of reaction tube's exit [3,10]. Also, our previous attempts to resublime GaN nanopowders towards large monocrystals under an ammonia flow at 1000–1100 °C for several hours have failed due to the major decomposition pathway with metallic Ga formation in the crucible (unpublished results).

This has to be compared with the drastically different nature and dynamics of mass losses observed for the similarly heated HVPE materials. Here, the comparable to nanopowders mass losses are

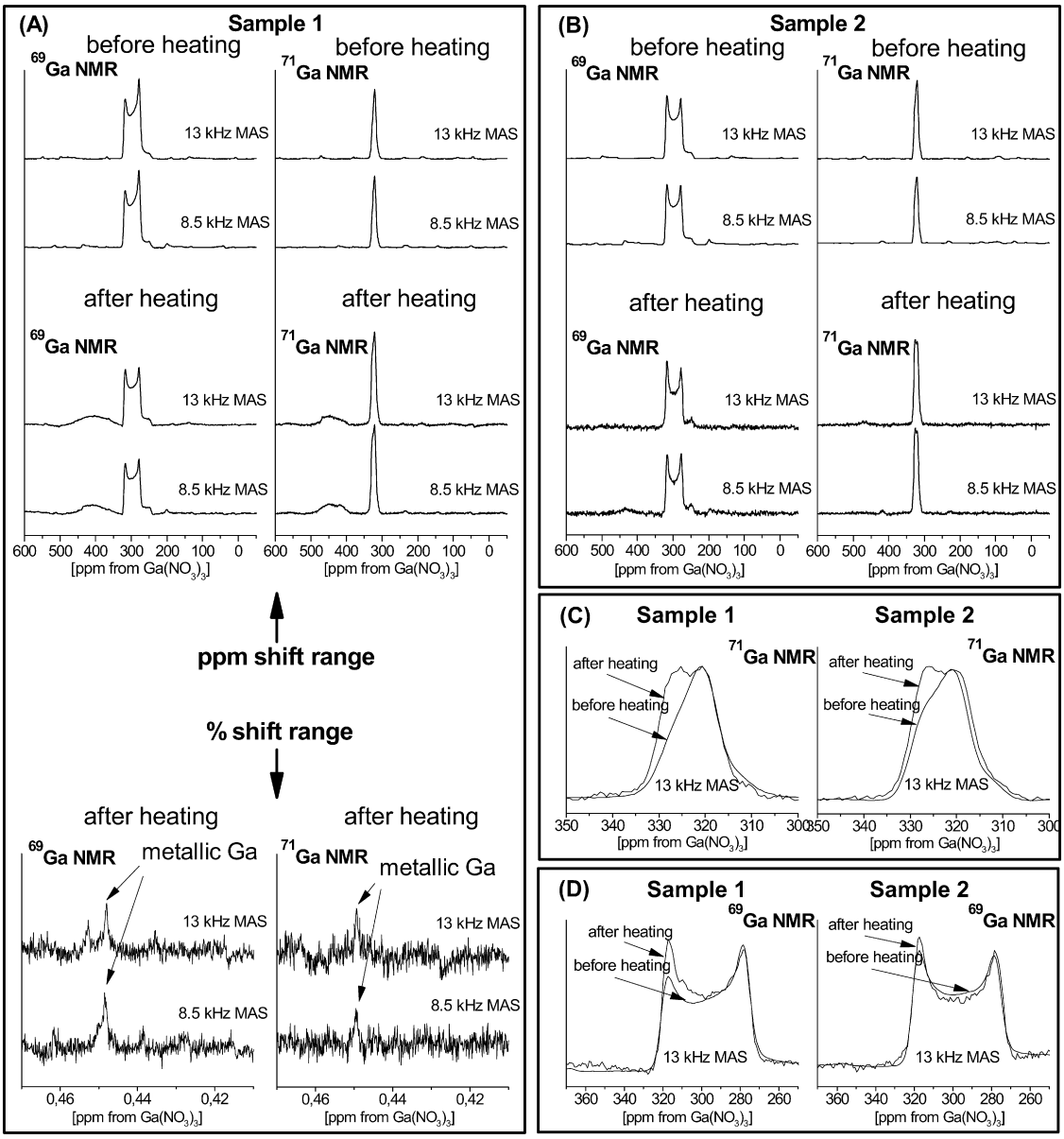

Fig. 4. ^{69}Ga and ^{71}Ga MAS NMR spectra for ground samples of HVPE GaN.

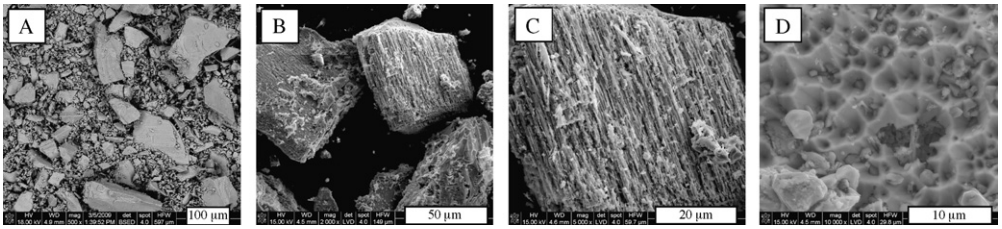

Fig. 5. SEM pictures of ground Sample 1. (A) Before heating and (B–D) after final heating.

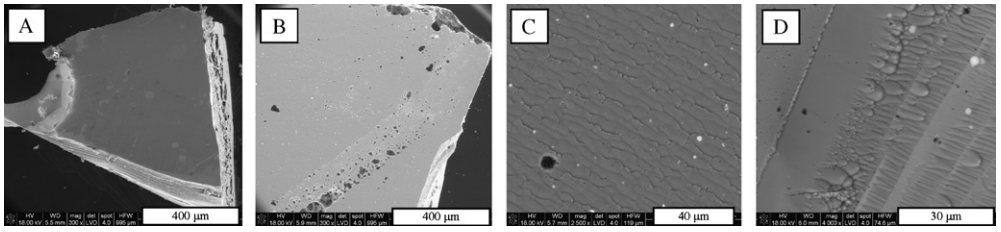

Fig. 6. SEM pictures of bulk sample 1 (platelet). (A) Before heating and (B–D) after final heating.

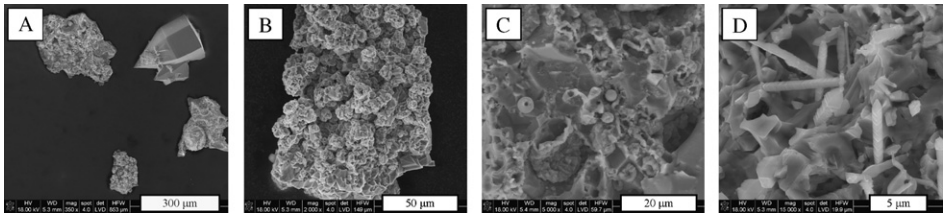

Fig. 7. SEM morphology of the deposits recovered from the reaction tube.

experienced at a much higher temperature of 1300 °C while the major pathway appears to be GaN sublimation accompanied by nitride decomposition mostly in the gas phase. The latter is supported by the observation that the deposits recovered from the tube areas above the heated samples in addition to resublimed crystalline GaN seem to contain metallic Ga and the black coloration of the reaction tube's exit supports the finely dispersed metal, too. In this regard, although after heating ground Sample 1 some minute quantities of metallic Ga are evidenced by NMR (no bulk metal was found in the crucible), no metal whatsoever is detected even after longer heating of Sample 2. It is also worth to notice that the relative rates of mass loss at 1300 °C of the HVPE GaN samples became visibly accelerated at some point of heating time. This can likely be linked to the lower and lower starting amounts and increased surface area of the remaining materials from the preceding stage both factors favoring better diffusion and more efficient mass transfer conditions operating in sublimation and/or decomposition.

However, the most striking observation is that related to the inappreciable size of the phenomenon responsible for the Knight shift in the gallium NMR study of the HVPE GaN samples as compared with the previously reported case of the GaN nanopowders [3]. In this regard, an additional weak Knight-shifted resonance in the *ca.* 410–430 ppm range is observed for heated ground Sample 1 while it is absent at all for heated ground Sample 2. Recall that the heating at 1300 °C of both HVPE materials was terminated by necessity after the abrupt mass loss yielded, eventually, minute quantities of the remaining products. This has to be compared with such a high-frequency Knight-shifted resonance often dominating over the lower-frequency resonance in the *ca.* 300 ppm range (stoichiometric Ga(4N) chemical environments) for many nanopowders, especially, those synthesized or heated for prolonged times at the temperatures of 975–1000 °C that define the thermal stability range of nanocrystalline GaN.

Looking more closely at the phenomena operating near the different thermal stability ranges for these two materials forms, we can conclude the following. First, the ammonia atmosphere appears to stabilize the nitride both in the bulk solid phase and the sublimed gas phase up to the relatively high temperatures, likely, by virtue of being a source of an additional *in situ* formed reactive nitrogen [1]. This can be compared with an inert gas atmosphere of helium resulting in the abrupt decomposition to the elements at significantly lower temperatures. Second, the interplay of sublimation and decomposition to the elements under ammonia has a specific pattern for the two hexagonal materials forms. The decomposition seems to be especially pronounced for the nanopowders with noticeable metallic Ga formed in the crucible already around 1000 °C while for the microcrystalline materials it takes part rather in the gas phase effecting the sublimed out species at some 1250–1300 °C. For the latter form, the sublimation along certain crystallographic axes is preferred. And, third, the major phenomenological difference between the nanopowders and microcrystalline powders of ground HVPE GaN at appropriately high temperatures is a pronounced crystal growth/recrystallization occurring in the bulk of the former and being only residual if any for obvious reasons in the latter. The crystal growth can be envisioned as larger crystallites growing at the expense of the smallest ones, eventually, into the micrometer size range that in terms of powder XRD is commonly referred to as the better/improved crystallinity. Since, concurrently with applying critical high temperature conditions, the gallium NMR shows for the nanopowders increased magnitude of the Knight shift phenomenon (see, our previous study [3]), the high temperature-induced crystal growth/recrystallization is likely to be responsible for it. Sample 1 of HVPE GaN that shows a very weak Knight shift effect was apparently ground to finer fractions than Sample 2 and this could conduce some recrystallization of the finest grains. In other words, it is grain recrystallization that appears to favor native N-defect formation and/or impurity oxygen incorporation into the crystal lattice of GaN to produce conduction electrons in the nanocrystalline semiconductor. In contrast, there is no evidence that prolonged heating even at temperatures as high as 1250–1300 °C under comparable ammonia flow conditions results in the formation of any significant N-deficient phase/conduction electrons within the bulk of the microcrystalline powders of ground HVPE GaN. In regard to GaN nanopowders, it is a matter of another study to probe if any kind of gas specific high temperature annealing of the nanopowders showing the Knight shift effect in the gallium NMR could control this property, possibly, in a reversible way.

4. Conclusions

The microcrystalline samples of ground hexagonal GaN prepared by the HVPE method showed significantly different behavior at high temperatures under ammonia than previously observed for various GN nanopowders. They survived a several-hour heating at 1300 °C to be compared with the related stability range of 975–1000 °C for the nanopowders. Under the applied conditions, the HVPE GaN underwent mostly sublimation and some decomposition to the elements. The evolving morphology of the resulting grains indicated some preferred crystallographic directions of the changes responsible for mass losses. In striking contract to nanopowders, no significant formation of the N-deficient phase/conduction electrons responsible for the Knight shift effect in the ^{69}Ga and ^{71}Ga MAS NMR spectra was detected in the heated HVPE materials. The sometime prevailing Knight shift effect for suitably pyrolyzed GaN nanopowders could, therefore, reasonably be linked to specific crystal growth/recrystallization phenomena operating in such systems while being naturally absent or remnant in microcrystalline and monocrystalline materials.

Acknowledgement

JFJ wants to acknowledge a financial support of AGH-UST, task no. 11.11.210.120.

References

[1] (a) T.J. Peshek, J.C. Angus, K. Kash, J. Cryst. Growth 311 (2008) 185, and references therein;
(b) A.A. Wolfson, E.N. Mokhov, Semiconductors 43 (3) (2009) 400, and references therein;

(c) B. Kallinger, E. Meissner, P. Berwian, S. Hussy, J. Friedrich, G. Mueller, Cryst. Res. Technol. 43 (1) (2008) 14, and references therein.
[2] (a) S. Stelmakh, A. Swiderska-Sroda, G. Kalisz, S. Gierlotka, E. Grzanka, B. Palosz, M. Drygas, J.F. Janik, R.T. Paine, Poster, 1399 Proceedings of the International Conference on Nanoscience and Technology, Basel, Switzerland, July 30–August 4, Institute of Physics Publishing, Philadelphia, PA, 2006;
(b) E. Grzanka, S. Stelmakh, S. Gierlotka, A. Swiderska-Sroda, G. Kalisz, B. Palosz, M. Drygas, J.F. Janik, R.T. Paine, Presented at Powder Diffraction Conference, EPDIC-10, Geneva, Switzerland, September 1–4, 2006, Z. Kristallogr. 26 (2007) MS11–P92;
(c) J. Borysiuk, P. Caban, W. Strupinski, S. Gierlotka, S. Stelmakh, J.F. Janik, Cryst. Res. Technol. 42 (12) (2007) 1291.
[3] M. Drygas, Z. Olejniczak, E. Grzanka, M.M. Bucko, R.T. Paine, J.F. Janik, Chem. Mater. 20 (2008) 6816.
[4] (a) O.H. Han, H.K.C. Timken, E. Oldfield, J. Chem. Phys. 89 (10) (1988) 6046;
(b) W.-S. Jung, C. Park, S. Han, Bull. Korean Chem. Soc. 24 (7) (2003) 1011;
(c) W.-S. Jung, Mater. Lett. 60 (2006) 2954;
(d) B. Schwenzer, J. Hu, R. Seshadri, S. Keller, S.P. DenBaars, U.K. Mishra, Chem. Mater. 16 (2004) 5088;
(e) B. Schwenzer, J. Hu, Y. Wuc, U.K. Mishra, Solid State Sci. 8 (2006) 1193;
(f) J.P. Yesinowski, Phys. Status Solidi C 2 (7) (2005) 2399;
(g) J.P. Yesinowski, A.P. Purdy, H.Q. Wu, M.G. Spencer, J. Hunting, F.J. DiSalvo, J. Am. Chem. Soc. 128 (2006) 4952.
[5] (a) J.P. Yesinowski, A.P. Purdy, J. Am. Chem. Soc. 126 (2004) 9166;
(b) W.-S. Jung, O.H. Han, S.-A. Chae, Mater. Chem. Phys. 100 (2006) 199.
[6] (a) J.D. Stroud, S.L. Segel, J. Phys. F: Metal Phys. 5 (1975) 1981;
(b) D.A. Cornell, Phys. Rev. 153 (1) (1967) 208.
[7] (a) R. Groh, G. Gerey, L. Bartha, J.I. Pankove, Phys. Status Solidi A 26 (1974) 353;
(b) J.Y. Li, X.L. Chen, Z.Y. Qiao, Y.G. Cao, Y.C. Lan, J. Cryst. Growth 213 (2000) 408;
(c) H.-D. Xiao, H.-L. Ma, Z.-J. Lin, J. Ma, F.-J. Zong, X.-J. Zhang, Mater. Chem. Phys. 106 (2007) 5;
(d) J. Unland, B. Onderka, A. Davydov, R. Schmid-Fetzer, J. Cryst. Growth 256 (2003) 33.
[8] (a) V. Darakchieva, B. Monemar, A. Usui, M. Saenger, M. Schubert, J. Cryst. Growth 310 (2008) 959;
(b) C.M. Balkas, C. Basceri, R.F. Davis, Powder Diffr. 10 (4) (1995) 266;
(c) W. Paszkowicz, S. Podsiadlo, R. Minikayev, J. Alloys Compd. 382 (2004) 100, and references therein.
[9] D. Freude, J. Haase, in: P. Diehl, et al. (Eds.), NMR of Quadrupolar Nuclei in Solids. NMR Basic Principles and Progress: Special Applications, vol. 29, Springer-Verlag, New York, 1993, pp. 1–90.
[10] J.F. Janik, M. Drygas, S. Stelmakh, E. Grzanka, B. Palosz, R.T. Paine, Phys. Status Solidi A 203 (6) (2006) 1301.